AGU PUBLICATIONS
JGR
Journal of Geophysical Research: Space Physics

RESEARCH ARTICLE
10.1002/2014JA019955

Key Points:
- Solar wind and magnetosphere parameters predict relativistic electron flux
- Multiple regression analysis is used to control for correlated predictors
- High levels of flux following storms are best modeled by a set of variables

Correspondence to:
L. E. Simms,
simmsl@augsburg.edu

Citation:
Simms, L. E., V. Pilipenko, M. J. Engebretson, G. D. Reeves, A. J. Smith, and M. Clilverd (2014), Prediction of relativistic electron flux at geostationary orbit following storms: Multiple regression analysis, *J. Geophys. Res. Space Physics*, *119*, 7297–7318, doi:10.1002/2014JA019955.

Received 9 MAR 2014
Accepted 12 AUG 2014
Accepted article online 15 AUG 2014
Published online 18 SEP 2014

Prediction of relativistic electron flux at geostationary orbit following storms: Multiple regression analysis

Laura E. Simms[1], Viacheslav Pilipenko[2], Mark J. Engebretson[1], Geoffrey D. Reeves[3], A. J. Smith[4], and Mark Clilverd[5]

[1]Physics Department, Augsburg College, Minneapolis, Minnesota, USA, [2]Institute of the Physics of the Earth, Moscow, Russia, [3]Los Alamos National Laboratory, Los Alamos, New Mexico, USA, [4]VLF ELF Radio Research Institute, Bradwell, UK, [5]British Antarctic Survey, Cambridge, UK

Abstract Many solar wind and magnetosphere parameters correlate with relativistic electron flux following storms. These include relativistic electron flux before the storm; seed electron flux; solar wind velocity and number density (and their variation); interplanetary magnetic field B_z, *AE* and *Kp* indices; and ultra low frequency (ULF) and very low frequency (VLF) wave power. However, as all these variables are intercorrelated, we use multiple regression analyses to determine which are the most predictive of flux when other variables are controlled. Using 219 storms (1992–2002), we obtained hourly averaged electron fluxes for outer radiation belt relativistic electrons (>1.5 MeV) and seed electrons (100 keV) from Los Alamos National Laboratory spacecraft (geosynchronous orbit). For each storm, we found the $\log_{10}$ maximum relativistic electron flux 48–120 h after the end of the main phase of each storm. Each predictor variable was averaged over the 12 h before the storm, the main phase, and the 48 h following minimum *Dst*. High levels of flux following storms are best modeled by a set of variables. In decreasing influence, ULF, seed electron flux, *Vsw* and its variation, and after-storm B_z were the most significant explanatory variables. *Kp* can be added to the model, but it adds no further explanatory power. Although we included ground-based VLF power from Halley, Antarctica, it shows little predictive ability. We produced predictive models using the coefficients from the regression models and assessed their effectiveness in predicting novel observations. The correlation between observed values and those predicted by these empirical models ranged from 0.645 to 0.795.

1. Introduction

Fluxes of energetic electrons (kinetic energy > 1.5 MeV) in Earth's outer radiation belt near geostationary orbit may show considerable fluctuations during and following geomagnetic storms [*Reeves*, 1998]. While there may be a rapid decrease in flux during the main phase of a storm, presumably due to an adiabatic response to magnetic field changes [*Kim and Chan*, 1997; *Green and Kivelson*, 2001], there is often a dramatic, if gradual, increase during the recovery phase. It is these dramatic increases that are of concern, as very high levels of energetic electrons can damage sensitive electronic components of satellites and disrupt such important services as communications and weather observations [*Baker et al*., 1987, 1998a; *Lanzerotti*, 2001; *Pilipenko et al*., 2006].

However, these recovery phase increases occur only after ≈50% of storms, and the amount of the increase is not well correlated with the strength of the storm [*Reeves et al*., 2003; *Reeves*, 1998]. In some storms, the electron flux never climbs as high as pre-storm levels [*Onsager et al*., 2002; *O'Brien et al*., 2001]. Clearly, other factors must be at play than just the strength of each storm as measured by the *Dst* drop.

Numerous studies have documented correlations between flux enhancements at geostationary orbit and factors in the solar wind and magnetosphere beyond the simple metric of the *Dst* drop. Solar wind velocity was the first correlate described [*Paulikas and Blake*, 1979]. This positive correlation between wind velocity and flux has been noted many times since [*Blake et al*., 1997; *Baker et al*., 1998b; *O'Brien et al*., 2001; *Reeves et al*., 2003; *Weigel et al*., 2003; *Ukhorskiy et al*., 2004; *Lyons et al*., 2005; *Lyatsky and Khazanov*, 2008a, 2008b; *Reeves et al*., 2011; *Kellerman and Shprits*, 2012; *Potapov et al*., 2012, 2014] and has been used to model flux levels [*Baker et al*., 1990; *Li et al*., 2001; *Vassiliadis et al*., 2002]. In addition, the variation in solar wind is well correlated with electron flux [*Potapov et al*., 2012, 2014].

Substorm activity (as measured by *AE*) following storms is also related to an increased flux [*Baker et al*., 1990; *Meredith et al*., 2003; *Li et al*., 2009], and both seed electron flux [*Hwang et al*., 2004] and energetic electron flux prior to the storm [*Reeves et al*., 2003] show a correlation with energetic electron flux in recovery. The previous day's electron flux is also well correlated with current electron flux when all days (both quiet and disturbed) are studied [*Ukhorskiy et al*., 2004].

Correlations have also been found with various geomagnetic indices such as *Dst*, *Kp*, *SYM-H*, and *PC* [*Baker et al*., 1990; *Dmitriev and Chao*, 2003; *Lyatsky and Khazanov*, 2008b; *Ukhorskiy et al*., 2004]. Interplanetary magnetic field (IMF) direction is another factor found to be influential [*Blake et al*., 1997; *Iles et al*., 2002; *Miyoshi and Kataoka*, 2008; *Miyoshi et al*., 2013], although the variation in IMF B_z is not as significant [*Potapov et al*., 2012]. There is generally a negative correlation with solar wind number density [*Lyatsky and Khazanov*, 2008b; *Balikhin et al*., 2011; *Kellerman and Shprits*, 2012; *Potapov et al*., 2012]. Electric field oscillations [*Tan et al*., 2011] show a correlation with electron flux enhancement, although it is possible that this can be explained by the correlations with solar wind speed and IMF B_z, which are themselves highly correlated with the electric field. Similarly, a correlation with solar wind pressure [*Tan et al*., 2011] may be explained by the correlations with solar wind velocity and number density.

Whistler mode chorus waves (VLF) have been postulated to be a factor in the acceleration of seed electrons to relativistic energies. Numerous studies have modeled flux enhancements using VLF waves, getting good agreement between observed flux and that predicted by the observed VLF [e.g., *Albert et al*., 2009; *Tu et al*., 2014]. Statistical studies have also found an association between an increase in VLF activity and relativistic electron enhancement following the minimum *Dst* [*Meredith et al*., 2003; *O'Brien et al*., 2003; *Smith et al*., 2004; *Miyoshi et al*., 2013]. More evidence comes from satellite observations of the VLF waves leading directly to relativistic electron flux enhancement in single storms [*Horne et al*., 2005; *Thorne et al*., 2013; *Li et al*., 2014; *Su et al*., 2014; *Turner et al*., 2014; *Xiao et al*., 2014].

Lastly, the level of ULF (ultra low frequency) wave activity is positively correlated with flux [*Rostoker et al*., 1998; *Mathie and Mann*, 2000; *O'Brien et al*., 2003; *Kozyreva et al*., 2007; *Potapov et al*., 2014]. This is true of both toroidal ULF waves and compressional poloidal ULF waves [*Tan et al*., 2004, 2011], although more poloidal and compressional wave power than toroidal has been observed during the recovery phase of high electron flux events [*Clausen et al*., 2011]. *O'Brien and McPherron* [2003] postulated ULF wave power, along with *Dst*, as one of the main drivers of electron acceleration in their model. *Elkington* [2006] reviews further studies suggesting ULF wave activity accelerates electrons to high energies.

However, it is not clear from simple correlation analyses whether each parameter is independently correlated with increases in relativistic electron flux. Disturbances in the magnetosphere are manifested as a rise in activity in many parameters. Only a few may actually correlate well with relativistic electron enhancements when other variables are held constant. Many of the variables thought to influence relativistic electron flux have been found to be correlated among themselves [*Lyons et al*., 2005; *Simms et al*., 2010; *Potapov et al*., 2012]. This intercorrelation of possible causative variables has led researchers to propose models where several parameters act simultaneously to produce enhancements of relativistic electrons. *Miyoshi and Kataoka* [2008] studied the joint effect of solar wind velocity and IMF B_z direction during periods of high-speed solar wind streams, finding that wind speed by itself was not enough to cause flux enhancements. Southward IMF B_z coupled with high wind velocity was followed by flux increases. *Lyatsky and Khazanov* [2008b] analyzed the effect of solar wind number density when velocity was held constant by examining the correlation between solar wind number density and relativistic electron flux during periods when velocity was low. Using this method, they found that number density had an independent negative correlation with flux. Highest fluxes, therefore, occurred following periods of high geomagnetic activity and low number density. *Kellerman and Shprits* [2012] refined the study of the joint effect of velocity and density by controlling for each variable using 2-D probability distribution functions. They found that flux depends on both variables simultaneously. *Ukhorskiy et al*., [2004] used even more predictors in a multivariable analysis, finding that solar wind velocity, the *SYM-H* index, and a lag term of the previous day's flux described the observed flux well. In this model, the predicted flux was dominated by the lag term: fluxes tend to remain relatively constant over periods longer than 1 day. However, the addition of *SYM-H* and velocity each contributed to the prediction. Pressure and convective electric field (solar wind velocity times the southward component of the interplanetary magnetic field) were also tested, but they contributed much less. Using an error reduction ratio analysis,

Balikhin et al. [2011], in contrast to the above studies, found more dependence on number density than velocity or B_z, with higher fluxes occurring in response to low density. Finally, *Li et al*. [2011], by examining the correlation of their model output with data from several years, determined that flux could best be predicted by a combination of velocity, IMF orientation, and the *Dst* index, although the *Dst* is itself the product of solar wind parameters.

As many previous multivariable studies span entire years or even decades, they do not specifically address the question of what factors are responsible for the largest relativistic electron flux increases following geomagnetic disturbances. Long stretches of geomagnetically quiet periods are contrasted with bursts of active periods. Thus, while these studies show that factors often associated with a disturbance (*Dst* drop, velocity rise, etc.) are correlated with flux increases, they do not focus specifically on which factors correlate best with the largest flux increases. There may be essential differences between disturbances that produce a high level of flux and those that produce only a modest increase above that seen in quiet times. These differences would not be seen in an overall study dominated by the large-scale division into quiet and disturbed times.

However, the studies that do look at storm times in particular are single-factor studies. Thus, a multifactor analysis of the causes of flux increases following storms alone is important. In the current study, we use a database of geomagnetic disturbances spanning the years 1992–2002. By removing quiet periods over this span of years, we are able to determine which factors play a role in whether a disturbance is followed by a rise in flux or not.

In contrast to previous multivariable studies, we use the technique of multiple regression, which allows the straightforward addition of more predictor variables to the analysis, as well as determining which predictors are most significant when all other factors are held constant [*Neter et al*., 1985; *Simms et al*., 2010; *Golden et al*., 2012]. This allows us to add seed electron levels and ULF and VLF waves to our analyses, expanding on earlier multivariable studies which considered only a few solar wind parameters and geomagnetic indices. However, some variables which are explicitly dependent on others, such as solar wind pressure which is dependent on velocity and number density, may only be added to these models if the variables they are derived from are removed. In this case, decisions about which to include can be based on the predictive ability of the resulting model or on a desire to test certain hypotheses about the mechanisms increasing electron flux. These analyses, at heart, are merely correlation studies. In a strict sense, therefore, results of these analyses may only be said to useful in predicting flux, not in determining which variables physically drive the flux increases. However, models such as these are useful in developing or disproving hypotheses about whether particular variables could be drivers, as a variable that shows no relationship to flux is unlikely to be a physical process that drives flux increases.

We remind readers that the 11 year relativistic electron flux database used here was obtained at geostationary orbit. Recent observations by the two Van Allen Probes spacecraft launched in 2012, which cover the range of radiation belt locations out to 5.8 R_E, do not overlap the part of the outer radiation belt studied in this paper.

2. Methods

We identified 219 storms (1992–2002) with at least 72 storm-free hours after the end of recovery (when *Dst* returns above −30 nT). We used the criteria of minimum *Dst* less than −30 nT and minimum B_z less than −5 nT to select events. We obtained hourly averaged electron fluxes for relativistic electrons (>1.5 MeV) and seed electrons (100 keV) from several spacecraft (Los Alamos National Laboratory (LANL)) energetic particle instruments in geosynchronous orbit (approximately 6.6 R_E). No spacecraft was in operation for this entire period, so we averaged over all available satellites in each hour. As each satellite was calibrated differently, we first converted each observation to a standardized score with mean 0 and standard deviation of 1 using the following formula:

$$\text{Standardized Observation} = \frac{\text{observation} - \text{mean of satellite}}{\text{standard deviation of satellite}} \quad (1)$$

We then found the maximum relativistic electron flux of these hourly averages in the 48–120 h following each storm. For some storms, this period was shorter than 120 h because the next event began before this 5 day period ended. However, much of the rise in flux occurs within 72 h of the end of the storm.

As predictor variables, we used a ground-based ULF index [*Kozyreva et al*., 2007] (2–7 mHz, covering local times 0500–1500) or ULF measured by the GOES satellite (covering the full 24 h period) and Halley VLF. We used the 1.0 kHz VELOX channel of Halley VLF (includes frequencies from 0.5 to 1.5 kHz) as it showed the most influence in simple correlations and the multiple regressions. All wave power variables were $\log_{10}$ values. In addition, we obtained *AE*, *Kp*, IMF B_z, solar wind velocity (V_x in GSE coordinates), number density (*N*), variation in *V* (σV of total velocity), variation in *N* (σN), and pressure (*P*) from the Omniweb database, as well as the maximum of $\log_{10}$ of main phase seed electron (100 keV) and pre-storm relativistic electron (>1.5 MeV) fluxes. The variation in *V* and *N* (σV and σN) were standardized by dividing by *V* and *N*, respectively.

We found the average of each predictive variable during three storm phases: pre-storm (12 h before the *Dst* drop), main phase (from first *Dst* drop until minimum *Dst*), and after the storm (the 48 h following minimum *Dst*). In addition, we used the maximum solar wind number density during pre-storm and main phase (N Shock), and the storm minimum *Dst* and IMF B_z. For the multiple regression analyses, all variables were converted to rankit normal scores [*Sokal and Rohlf*, 1995] by replacing the rank of each observation by the position, in standard deviation units, of the ranked items in a normally distributed sample of the same *n*. This transformation gives a normal distribution, which allows the use of statistical tests that depend on normality.

We performed both simple and partial correlations of the relativistic electron flux with each predictor variable. Partial correlations were obtained by correlating between two variables of interest after excluding the effect of all other predictor variables. Using all possible predictor variables results in low partial correlations, as the correlations between predictor variables tend to be high. Additionally, using highly correlated independent variables in a multiple regression reduces the robustness of the model in its ability to reliably predict the relationship between predictors and the dependent variable [*Farrar and Glauber*, 1967]. A model with all possible variables entered may not reliably show the true relationship between predictors and flux.

A more informative, and statistically robust, approach would only keep variables as needed to obtain the maximum possible explanation of the flux response. To accomplish this, we used the method of backward elimination (a type of stepwise regression) to choose only the most explanatory variables. This method adds all variables to the model at the beginning then drops those which show no significant effect [*Hocking*, 1976]. After each variable is removed, a regression is run again with the reduced set, and the next variable that does not meet the criterion for inclusion dropped. The algorithm stops when all remaining predictor variables meet the significance criterion. We set the level at which to remove a variable at $p > 0.10$. This method is a means of producing a model that is not overfitted, while retaining all variables that show an influence.

As we were interested in building predictive models, we used only a semirandom sample of 80% ($n = 176$) of the storms to build the models. This left 20% ($n = 44$) of the storms to be used in validating the model. Storms were chosen by numbering all storms, eliminating all storms that were followed by subsequent storm activity in the next 3 days, and holding in reserve every storm whose number was divisible by 5. This gave a semi-random sample spread out over all years and seasons, with four-fifths of the data used for the analysis and one fifth held in reserve for validation of the model. In four subsequent analyses, we eliminated a different fifth of storms, using these sets to determine how sampling affected prediction ability. Statistical analyses were performed in Statistical Package for the Social Sciences (SPSS) and IDL (Interactive Data Language).

3. Results

Relativistic electron flux at geostationary orbit rises after many storms, along with a number of other parameters of the solar wind and magnetosphere. Figure 1 shows the behavior of the flux and these other variables during a typical storm (23–28 May 2000). Much of the rise in flux occurs at the end of recovery, peaks a day or two after recovery, and may remain elevated for a number of days afterward. A diurnal variation occurs due to the spacecraft orbit, with peak fluxes observed near local noon [*Reeves et al*., 1998]. Many of the other variables rise or fall in association with the increased geomagnetic activity of the storm. These changes in the days or hours before the rise in flux may appear as if they are driving the flux response. Beyond the *Dst* and B_z drops that define the storm, concomitant increases in seed electrons, solar wind velocity, number density, pressure, ULF, VLF, *Kp*, and *AE* all might be postulated as predictors, possibly even causes, of the flux increase following this particular storm event.

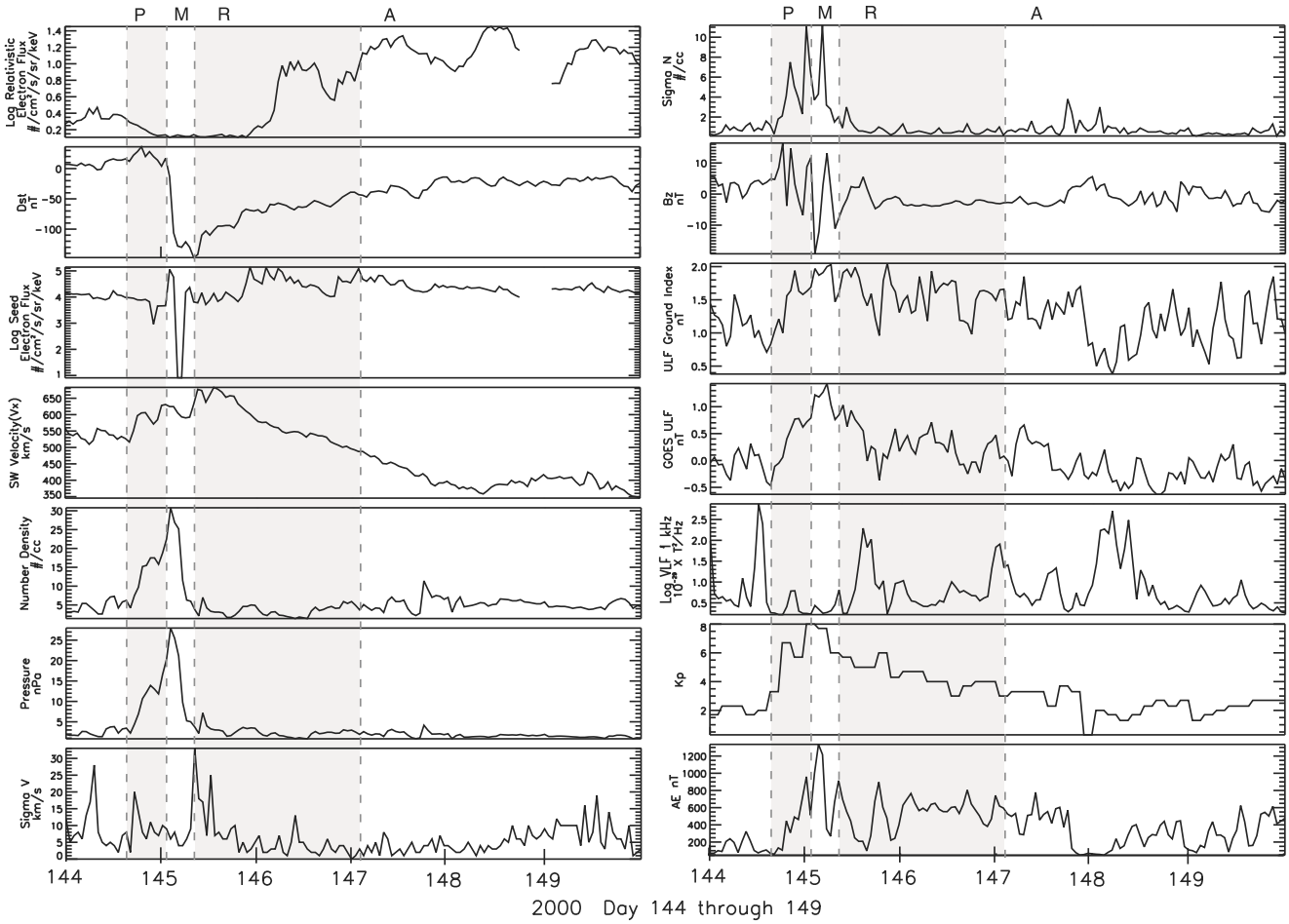

Figure 1. Time series plot, year 2000, days 144–149. Relativistic and seed electron fluxes are the standardized scores of the logs. P = pre-storm (12 h before main phase), M = main phase (from beginning of *Dst* drop to lowest *Dst*), *R* = 48 h after lowest *Dst* (period during which predictors variables after lowest *Dst* are averaged), *A* = 48–72 h after lowest *Dst* (period during which maximum flux is found).

Formal correlation analysis confirms this impression. Many of the other parameters are correlated with increased flux following storms (Figure 2). The first column of each panel gives the simple correlation of each possible predictor with flux. The highest simple correlations (above 0.5) occur with predictor variables following the minimum *Dst*. Both ground and satellite ULF, V_x, *AE*, and *Kp* after minimum *Dst* show strong correlations ($>$ 0.50). Ground ULF shows a stronger association than satellite ULF (0.65 versus 0.50). Average B_z following the main phase of the storm also shows a somewhat high correlation (-0.39) as does V_x (0.54) and the variation in V (0.26). Pressure is less associated (correlation of only 0.15), and VLF is not significantly correlated with relativistic electron flux.

During the main phase of the storm, V_x, seed electrons, the variation in *V*, and ground ULF show the strongest association with flux (correlations of 0.40, 0.37, 0.35, and 0.34, respectively). Again, the correlation with pressure is fairly low (0.13). Conditions during the pre-storm period are less influential. Although pre-storm *Kp* and *AE* correlations with flux are both significant, neither is particularly high (0.20). Pre-storm relativistic electrons show somewhat more association (0.25), and this may be an important factor in a predictive model as the relativistic electrons present before a storm may be part of the population of electrons afterward. Minimum storm *Dst* and B_z are even less predictive, showing correlations of -0.15 and 0.03, respectively.

However, many of these predictive factors are also correlated with each other (third column and onward of each panel of Figure 2). ULF (ground and satellite), *V*, IMF B_z, *Kp*, and *AE* are all strongly interassociated as well as being correlated with relativistic electron flux. Correlations between predictor variables can be high. For example, the V_x and ground ULF correlation is 0.73, while that of *AE* and *Kp* after the storm is 0.88. (The correlation

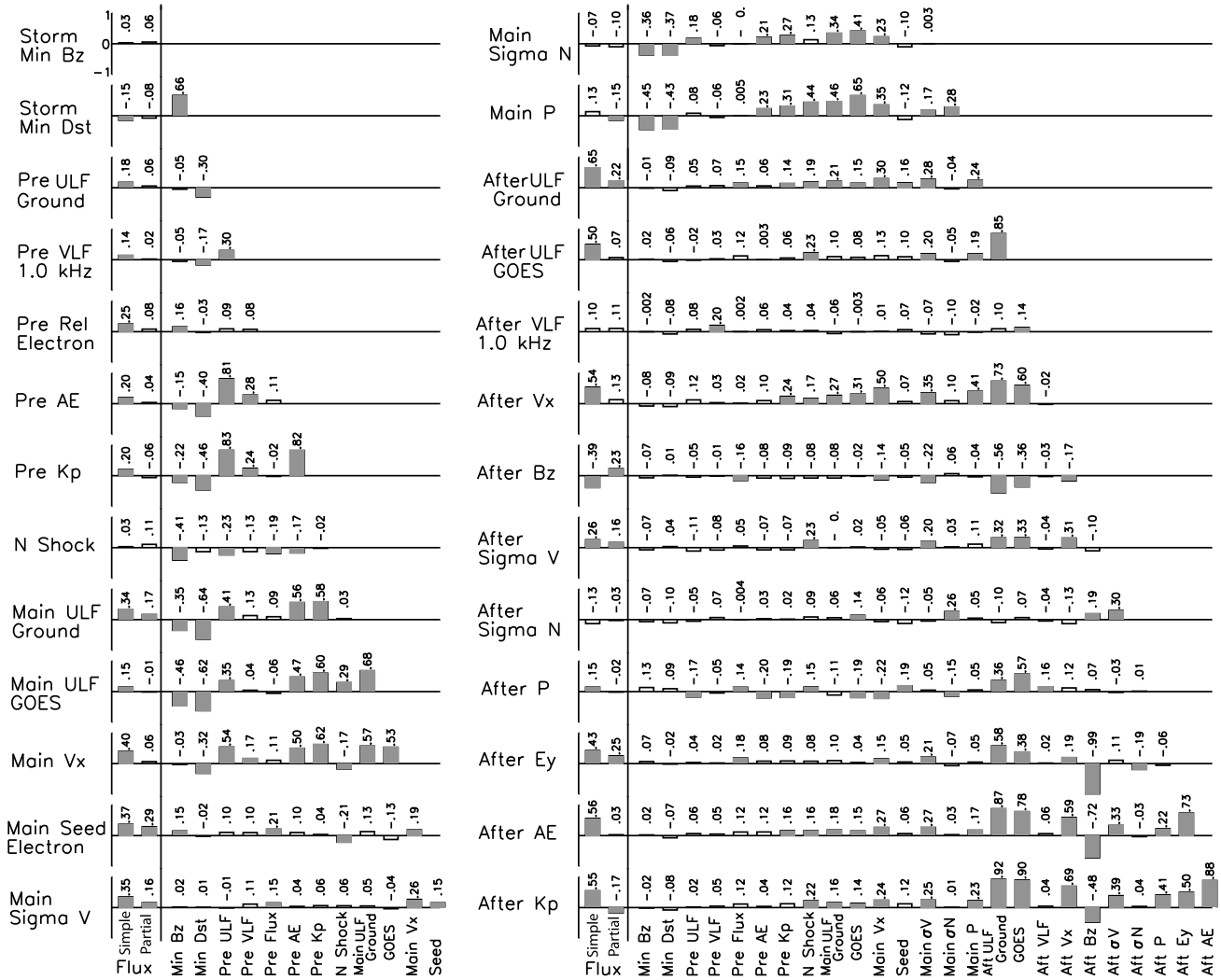

Figure 2. Correlations between relativistic electron flux and all predictor variables, and among all predictor variables. The first column of each panel is the simple correlation of each possible predicted variable with maximum relativistic electron flux following minimum *Dst*. The second column of each panel is the partial correlation between predictor and flux. Further columns are the pairwise correlations between predictor variables. This data set contains 219 storms. Significant correlations ($p < 0.05$) are given as solid bars; nonsignificant correlations are open bars. A correlation greater than 0.1325 is significant for the simple correlations (degrees of freedom = 218) and greater than 0.1405 is significant for the partial correlations (degrees of freedom = 193).

between after-storm B_z and E_y is nearly −1, but this is a consequence of E_y being mathematically derived from B_z.) Therefore, correlations between flux and each predictor variable may be covertly influenced by correlations between predictor variables. It is possible that only one of these predictors is responsible for the rise in flux, but its correlation with other possible predictors makes them all look as if they are drivers.

Partial correlation analysis holds other factors constant in the determination of the correlation between two variables. This gives some indication of whether explanatory variables are predictive of flux on their own or if they are only associated with other predictors. The partial correlations of each variable with flux are given in the second column of each panel of Figure 2. This correlation holds all other predictors constant, while giving the further association due to the one predictor in question. In most cases, the partial correlation of each predictor with flux is lower than the simple correlation. A number no longer have a significant influence when a full set of variables is controlled for. For some predictors, the correlation even switches sign (pre-storm and after-storm *Kp*, as well as main phase pressure).

Main phase seed electron flux, with a simple correlation of 0.37 and partial correlation of 0.29, maintains its influence even when other variables are controlled. This is also true of ground ULF

influence drops between simple and partial correlations (from 0.34 to 0.17 in main phase, 0.65 to 0.22 after minimum *Dst*), it still shows significant predictive ability. Satellite ULF (GOES) after minimum *Dst* shows a strong association with flux in the simple correlation (0.50) but loses almost all of this influence in the partial correlation (0.07). While satellite ULF (GOES) may be an acceptable predictor if ground ULF is not included, the addition of both causes the apparent influence of satellite ULF to fall. Both measurements of ULF (ground and satellite) describe very similar processes. Using both is not necessary. In the multiple regressions (below), we explore which might be the better predictor.

The simple correlation of V_x with flux in both main phase and after minimum *Dst* is considerable (Figure 2, first column: 0.40 and 0.54, respectively, both significant at $p < 0.05$), but the *Vx* influence is reduced when all variables are considered (Figure 2, second column: partial correlations of 0.06 and 0.13). This may well be due to the addition of σV, which also loses influence in the partial correlations (dropping from 0.35 to 0.16 in the main phase and less dramatically from 0.26 to 0.16 after minimum *Dst*). Both *Vx* and σV are likely explaining similar "parts" of a generalized effect of solar wind velocity on flux.

Other variables lose even more apparent influence. The simple correlation of pre-storm relativistic electron flux (0.25) drops to a partial correlation of 0.08. *AE* during the pre-storm interval drops from a simple correlation of 0.20 to a partial correlation of 0.04, while pre-storm *Kp* drops from 0.20 to −0.06. Storm minimum *Dst* with its low simple correlation of −0.15 also drops to −0.08 in the partial correlation. Pre-storm ground ULF shows a modest simple correlation (0.18), but the partial correlation drops to 0.06. Pre-storm VLF, similarly, has a simple correlation of 0.14, but a partial correlation of only 0.02. Pre-storm conditions and storm strength, in general, appear to have little influence on flux after the storm.

Conditions after minimum *Dst* correlate more closely with flux, although not always as expected. The simple correlation of B_z after minimum *Dst* (−0.39) switches the sign of its influence to 0.23 in the partial correlations. *Kp* and pressure correlations also switch the sign of their influence. *Kp*, with a simple correlation of 0.55, has a partial correlation of −0.17, while pressure simple correlations drop from 0.15 to −0.02. For *AE*, the high simple correlation of 0.56 drops to a partial correlation of 0.03.

Neither *N* nor σN shows much correlation with flux. However, the partial correlations shown here use all other possible predictors, including pressure. As pressure is intimately associated with *N*, the removal of it from the analyses may allow *N* or σN to show more influence. This will be shown below in the reduced regression models using GOES data. Ground VLF data, however, show little correlation in either simple or partial correlations. Minimum storm B_z also shows little influence in either simple or partial correlation.

These dramatic changes between simple correlations and partial correlations may be explained by the correlations that occur between predictor variables. Many are statistically significant. For example, the simple correlation of *Kp* and *AE* after minimum *Dst* with ground ULF is 0.92 and 0.87, respectively. *AE* and *Kp* are themselves correlated with an *r* of 0.88. Similar high correlations can be found between other variables, the most striking being a correlation of −0.99 between E_y and B_z after minimum *Dst*. These strong interrelationships make any conclusions based on simple correlations between each predictor and flux suspect.

3.1. Regression Analyses

Partial regression analysis is similar to partial correlation analysis in that it determines the effect of each variable when all others are held constant, but it also produces coefficients for each explanatory variable so that a predictive model can be produced. Figure 3 shows regression lines from both simple regression and partial regression between relativistic electron flux following minimum *Dst* (*y* axis) and selected untransformed predictor variables. Untransformed data are used in this figure so that the range of the actual observations can be seen, and so comparisons can be made to other studies. The simple regression lines do not align perfectly with the main cloud of points due to the presence of outliers. For example, in the main phase ULF plot, a few storms with high ULF but low flux (lower right of graph) skew the simple regression line downward. Removing these outliers would bring the regression line back into accordance with what seems to be the visual fit, but there is no evidence that these outliers are measurement mistakes. We must assume that they are valid observations and part of the phenomena that we hope to explain. That the partial regression lines show even less alignment with the main body of the points is only evidence that some of the correlation of each variable with flux is being explained by the other independent variables.

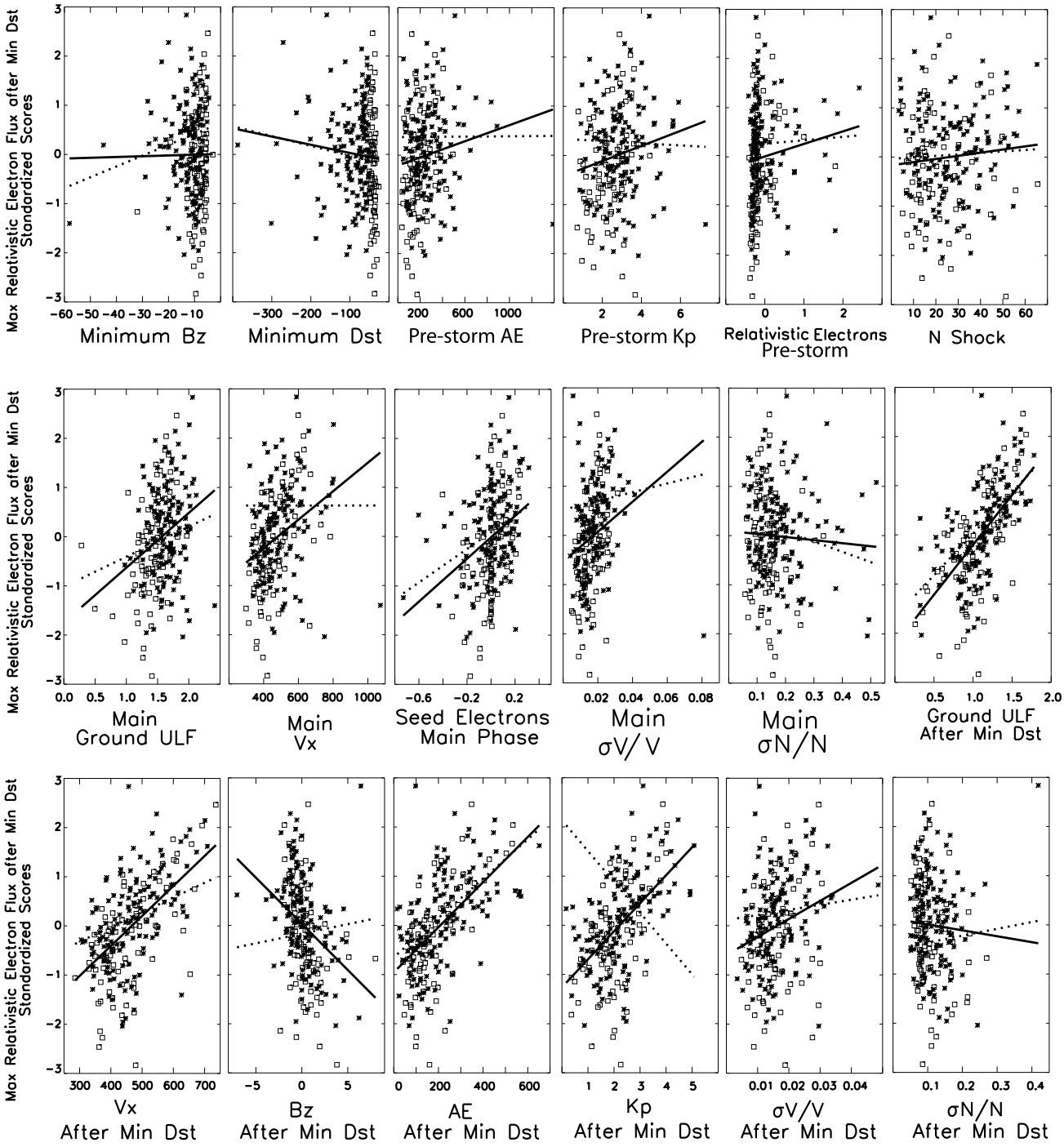

Figure 3. Scatterplots with simple (solid) and partial (dashed) regression slopes for selected untransformed predictor variables versus relativistic electron flux following minimum *Dst*. The partial regression coefficient is the effect of the given parameter when all other predictors are constant. For most predictor variables, the simple regression slope shows a stronger relationship than the partial regression. The slope switches direction of influence for several predictors. □ Minimum $Dst < -50$ * Minimum $Dst > -50$.

As with partial versus simple correlation, partial regression coefficients often show dramatically different slopes than those given by the simple regression coefficients. Scatterplots with simple (solid) and partial (dashed) regression slopes for selected predictor variables show that for most predictor variables, the simple regression slope shows a stronger relationship than the partial regression (where other predictors are held constant). The exceptions are storm minimum B_z and main phase sigma *N*. For some variables, their influence

Table 1. Addition of Variables One by One (Using Ground ULF), With Percent of the Variation in the Data Explained by Each[a]

	Percent of Variation Explained	Change in Percent Variation Explained	Simple Correlation With Flux
Ground ULF after minimum *Dst*	42.3%	42.3%	0.65
+*AE* after minimum *Dst*	42.3%	0.0%	0.56
+V_x after minimum *Dst*	43.2%	0.9%	0.54
+Main phase V_x	46.9%	3.7%	0.40
+IMF B_z after minimum *Dst*	47.3%	0.4%	−0.39
+Main phase seed electrons	53.2%	5.9%	0.37
+Main phase $\sigma V/V$	54.1%	0.9%	0.35
+Main phase ground ULF	55.6%	1.5%	0.34
+$\sigma V/V$ after minimum *Dst*	56.5%	0.9%	0.26
+Pre-storm relativistic electron flux	56.9%	0.4%	0.25
+Pre-storm *AE*	56.9%	0.0%	0.20
+Pre-storm ground ULF	57.0%	0.1%	0.18
+Minimum storm *Dst*	57.0%	0.0%	−0.15
+Pre-storm VLF	57.5%	0.5%	0.14

[a]Variables that have significant simple correlations are added in order of the magnitude of that correlation. (*Kp* is excluded for reasons explained in the discussion.)

is not seen unless other variables are held constant. The slope switches direction of influence for *Kp* (both pre-storm and after minimum *Dst*) and for sigma N and B_z after minimum *Dst*. For these, it may be that they are measuring very similar phenomena.

The scatterplots also show that there is no grouping of strong (*) or weak (□) storms showing low or high flux after the storm.

3.2. Model Building Through Multiple Regression

All predictor variables may be tested in a multiple regression model by entering all as independent parameters. However, problems of multicollinearity, in which some predictor variables are so highly correlated with each other, mean that not all variables can be entered in a regression model. With this in mind, we remove certain variables that are close proxies for one another from consideration. As pressure showed less relation with flux than solar wind velocity in the simple correlations, and as pressure and velocity are closely related, we chose to use only velocity and to drop pressure from our models. The correlation between GOES and ground ULF is similarly quite high, so we performed separate analyses including each of these. The relationship of *Kp* with flux is high, but, as seen in Figure 3, when all variables are included in the model, the effect of *Kp* becomes strongly negative. This led us to remove the *Kp* index from our next models, although we add it back in later for comparison. Lastly, we use only one VLF channel. Due to bandwidth overlap, the VLF channels are highly correlated. The 1.0 kHz band, for example, covers the range of 0.5–1.5 kHz, overlapping the 0.5 kHz band. These two channels have a correlation of 0.73. We chose to use only the 1.0 kHz band in the regressions, as it had the highest simple correlation with flux. However, we note that the ground-based VLF wave power from Halley, Antarctica, is a relatively localized measurement, not a global one, and is likely to only represent whistler mode chorus wave power for the few hours UT each day when it is in the morning magnetic local time sector. There are also strong seasonal effects, due to ionospheric attenuation in the summer months [*Smith et al.*, 2004]. This will be discussed in more detail in a study currently underway.

As the purpose of the regression analyses is to build a predictive model, we used only 80% of the storms to build these models, holding the remaining 20% in reserve for validation. We chose these storms for model validation by selecting every fifth storm.

That a multiple regression model can improve the fit to the data can be seen in Table 1. Here we build up the models by starting with ground ULF after the storm (the most significant simple correlation) and adding further variables in order of their simple correlation value. The percent of variation explained is the R^2 statistic (equivalent to the correlation coefficient squared). Although the ground ULF after minimum *Dst* can explain 42.3% of the variation in the data on its own, the addition of further variables can bring this to 57.5%. However, even though the variables are added in the order of magnitudes of their simple correlations, the increase in variation explained does not increase in proportion to these correlations. The simple correlations are not additive. The addition of *AE* and V_x after minimum *Dst* might be expected to add the most to the

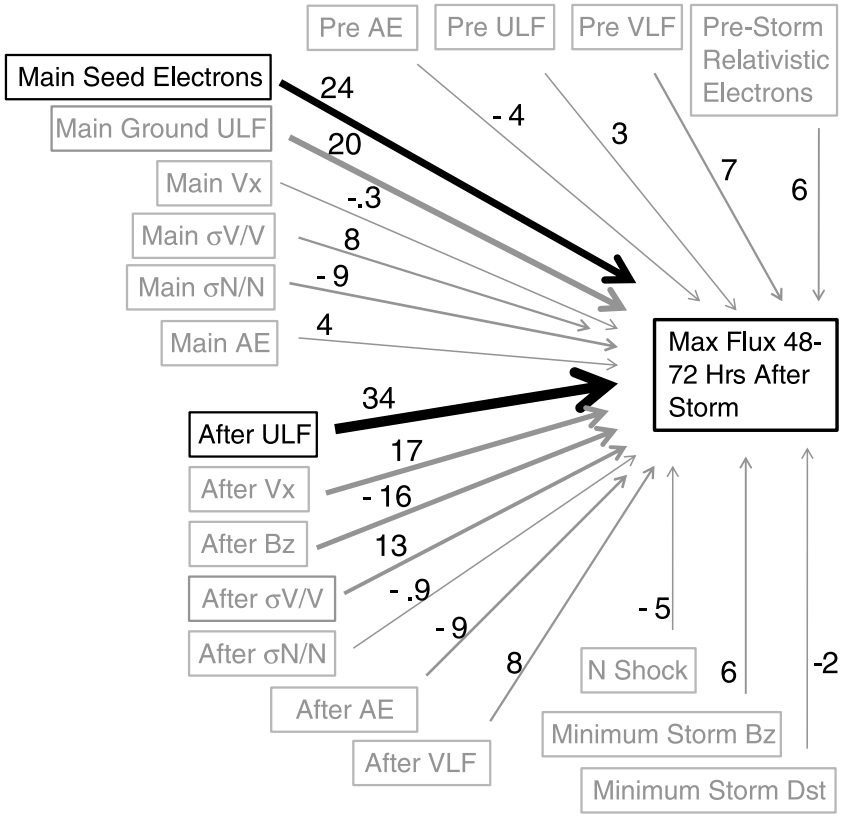

Figure 4. Relative influence of predictors in a full multiple regression model using ground ULF. Significant variables ($p < 0.05$) are in black. Numbers are the standardized regression coefficients × 100. Only two predictors show a significant relationship with flux. The coefficient of determination (R^2) of 0.59 means that 59% of the variation seen in the flux is explained. This is roughly equivalent to a correlation of 0.77. $n = 168$; roughly 80% of the data was used to build this model, holding the remaining 20% in reserve for model validation. Pre-storm values are averaged over the 12 h before the first *Dst* drop, "main" values are averaged between the first *Dst* drop to the minimum *Dst*, "after" values are averaged over the 48 h following the minimum *Dst*. Maximum relativistic electron flux is found 48–120 h after the minimum *Dst*.

percent variation explained, as they have the highest correlation after ground ULF, but they contribute little or nothing. The correlations of *AE* and *Vx* with ULF are both high; thus, neither *AE* nor V_x has little explanatory power to add beyond what has already been explained by ULF. In addition, the seed electron flux, which had only the fifth largest simple correlation, adds nearly six percentage points to the variation explained. Building a model by adding variables in the order of their simple correlation until the added percent variation explained became low would have stopped at one predictor: ground ULF. The later variables would never have been added.

The best model may not then be simply a model built up by adding the most influential variables as determined by their simple correlations. Some predictors seem to lie in a cluster, where one is a good proxy for the others, while other predictors influence flux independently. It may be worthwhile, therefore, to do a multiple regression which includes all the predictors to which we have access. Figure 4 shows the results of this full analysis using ground ULF with lines of influence showing the strength of the relationship of flux with each predictor. (Ground ULF, not GOES ULF is used, as the ground ULF index showed the highest simple correlation with flux.) Only two predictors show a significant relationship ($p < 0.05$) with flux in the full model: main phase seed electrons, and ground ULF after minimum *Dst*. The coefficient of determination (R^2) of 0.59 means that 59% of the variation seen in the flux is explained. This is roughly equivalent to a correlation of 0.77, the square root of R^2. In simple regression, the square root of the R^2 is the correlation coefficient, *r*.

Figures 2–4 present all or nothing cases, where either simple correlations or correlations/regressions accounting for many possible predictor variables are presented. Neither approach is likely the best. Although the influence of a particular variable may be reduced to a nonsignificant level when all other variables are included, this same variable may still show a significant effect when only a more reasonable subset of all possible variables are included.

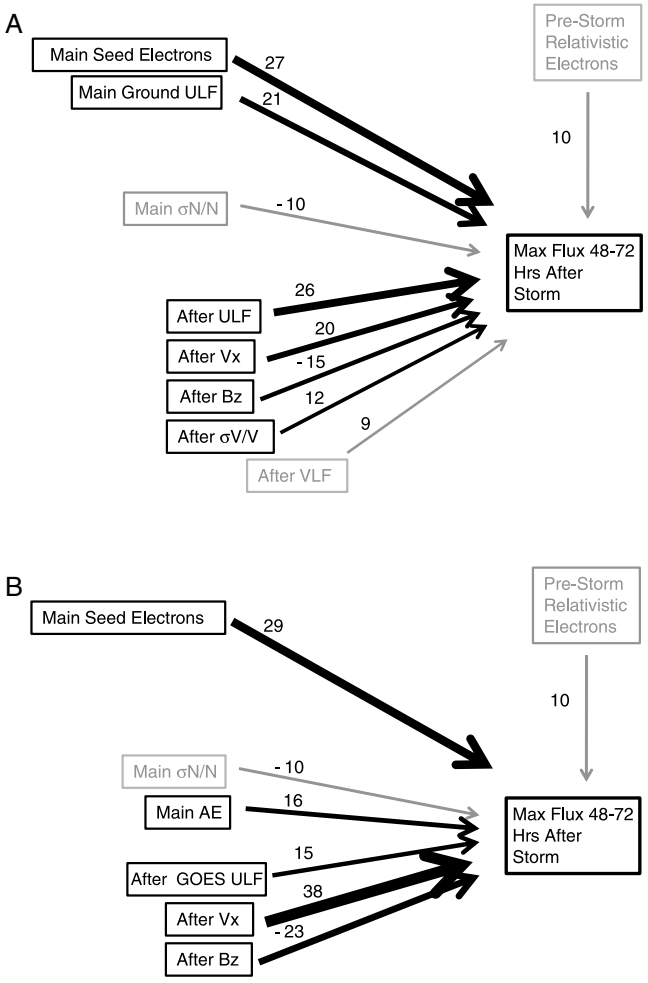

Figure 5. Relative influence of predictors in a multiple regression model reduced by backward elimination. (a) Ground ULF. (b) GOES ULF. A reduction in parameters results in increased influence of the remaining parameters, but the proportion of variation explained (56% and 52% for ground and GOES ULF, respectively) is only slightly lower. Factors were removed from the model if the p value was greater than 0.10. Significant predictors ($p < 0.05$) are in black; nonsignificant predictors ($p < 0.10$) are in gray. (This plot used approximately four-fifths of the data. One fifth was held in reserve for model validation. $N = 176$.)

3.3. Reduced Models by Backward Elimination

A full model, however, contains many variables which are intercorrelated. If the correlations between independent variables are strong, this will introduce multicollinearity to the model [*Neter et al.*, 1985]. Strong multicollinearity will increase the standard errors of the coefficients beyond acceptable limits. Inflated values for the standard errors will result in some independent variables wrongly judged to be not significantly different from zero—in other words, they will appear to have no influence. Thus, it is important to reduce the number of parameters in the model to the point where only significant and nearly significant variables are included. If the model is to be used for prediction, multicollinearity can introduce further difficulties. If too many highly intercorrelated variables are included in a model, it may not be particularly robust. Its predictive ability with another data set may be low compared to the predictive ability of a more parsimonious model that only includes a subset of predictors that are chosen for their ability to improve the fit of the model without a large increase in multicollinearity [*Chatterjee et al.*, 2000].

A more parsimonious model may be developed with the use of the backward elimination selection technique. This method starts with a full multiple regression model containing all the variables. At each step, the least significant variable is removed, until only significant variables remain. Results from this method are presented in Figure 5a (ground ULF index). The reduced model, while removing some parameters that are of very little influence, results in more parameters showing a significant effect. Seed electrons and ULF following the minimum *Dst* retain their significance in the reduced model, but further variables are now significant. Main phase ULF and variation in N, and V_x, the variation in V, and B_z after minimum *Dst* are retained as significant influences in the model. Pre-storm relativistic electrons ($p = 0.069$) as well as VLF following minimum *Dst* ($p = 0.098$) do not meet the $p < 0.05$ criterion of significance, but they are retained in the model by the process as the criterion for removal is $p > 0.10$. Although these two variables do not reach significance with this particular data set, they may be worth retaining in the model as they may be useful in prediction. Despite the reduction in variables from the full model, the proportion of variation explained is still 56% (roughly equivalent to a correlation of 0.75). This is evidence that the variables removed were of little value in prediction.

We also produced a reduced model using GOES satellite ULF instead of the ground ULF index (Figure 5b). This model includes main phase seed electrons and *AE*, as well as ULF, V_x, and B_z after minimum *Dst* as

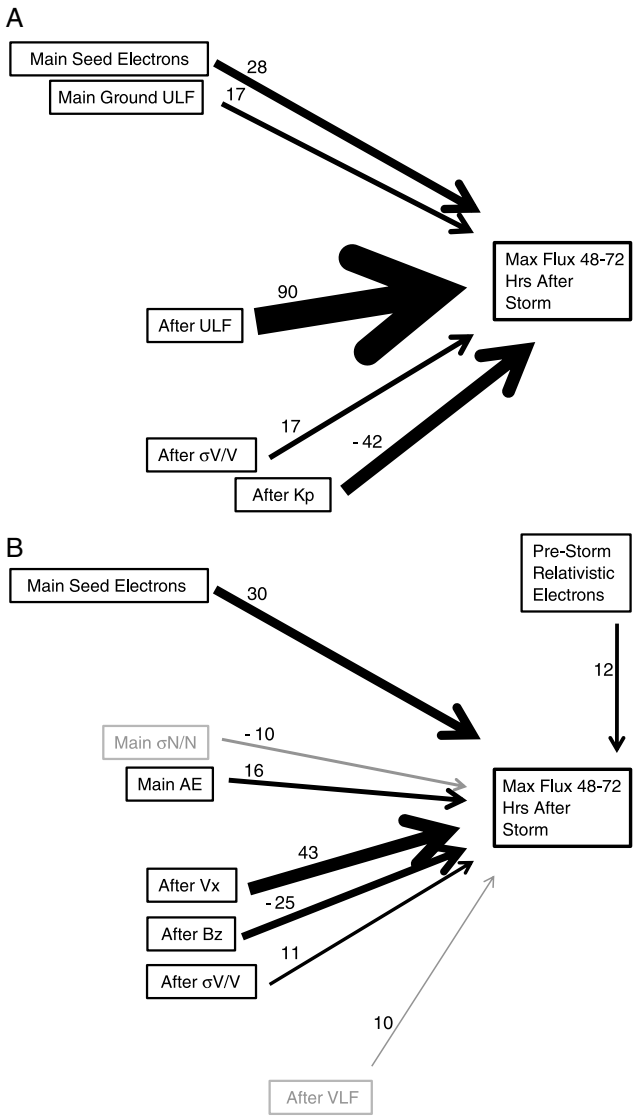

Figure 6. Relative influence of predictors in a multiple regression model with *Kp* as a possible predictor, reduced by backward elimination. (a) With ground ULF as a possible predictor. (b) Without ULF as a predictor. *Kp* has a strong negative effect, countered by a large increase in the ULF effect when ULF is a possible predictor. However, the percent of variation explained is slightly less than models without *Kp* (55% in Figure 6a). When ULF is not present, *Kp* itself is removed by the backward elimination (percent of variation explained = 53% in Figure 6b). Factors were removed from the model if the *p* value was greater than 0.10. Significant predictors ($p < 0.05$) are in black; nonsignificant predictors ($p < 0.10$) are in gray. $N = 176$.

significant influences. Although not statistically significant, main phase variation in *N* is retained in the model ($p = 0.058$). The amount of variation explained by the model is 52% (a correlation of roughly 0.72).

3.4. Addition of *Kp* to the Reduced Model

When the *Kp* index is added to the possible variables the backward elimination can choose from, it exhibits a strong negative influence (Figure 6a). However, this is concurrent with a large increase in the apparent ULF influence. B_z after minimum *Dst* is dropped from the model. The percent of variation explained by this model is 55% ("*r*" = 0.74), less than the reduced model without *Kp*. *Kp* appears to be a proxy for the variables that were dropped from this model, as well as working against the influence of after-storm ground ULF.

The opposing action of *Kp* and ULF suggests that an acceptable model might be developed using *Kp* without ULF. This was attempted (Figure 6b), but the resulting model not only explained less of the variation (53%, "*r*" = 0.73), *Kp* itself was removed by the backward elimination process. After-storm V_x and B_z become much more influential. Their high correlation with ULF allows them to explain some of the variation previously explained by ULF.

3.5. Model Validation

Each of the above regression models can be represented by either the standardized coefficients (given in the figures) which show the relative influence of each variable or by the unstandardized coefficients which can be used to produce a predictive model. The coefficients from these models are given in Table 2. As an example, the predictive model for the reduced model using ground ULF can be written as

$$\begin{aligned}\text{Rel Flux Following Storm} = &-0.028 + 0.104 \times (\text{Pre-storm Rel Flux}) + 0.287 \times (\text{Main Seed Electron Flux}) \\ &+ 0.210 \times (\text{Main Phase ULF}) + (-0.100) \times (\text{Main Phase } \sigma N/N) \\ &+ 0.258 \times (\text{After Storm Ground ULF}) + (-0.149) \times (\text{After Storm } B_z) \\ &+ 0.208 \times (\text{After Storm } V_x) + 0.121 \times (\text{After Storm } \sigma V/V) \\ &+ (0.087) \times (\text{After Storm VLF})\end{aligned} \quad (2)$$

Table 2. Unstandardized Regression Coefficients Used to Produce Predictive Models[a]

	Figure 4 Ground ULF Full Model, No *Kp*	Figure 5a Ground ULF Reduced Model, No *Kp*	Figure 5b GOES ULF Reduced Model, No *Kp*	Figure 6a Ground ULF Reduced Model With *Kp*
Constant	−0.035	−0.028	−0.029	−0.040
Minimum *Dst*	−0.019			
Minimum B_z	0.058			
N shock	−0.056			
Pre-storm relativistic electron	0.064	0.104	0.109	
Pre-storm ground ULF	0.032			
Pre-storm ground VLF	0.055			
Pre-storm *AE*	−0.041			
Pre-storm *Kp*				
Main seed electrons	0.258	0.287	0.316	0.298
Main ground ULF	0.201	0.210		0.178
Main GOES ULF				
Main V_x	−0.003			
Main $\sigma V/V$	0.085			
Main $\sigma N/N$	−0.087	−0.100	−0.099	
Main *AE*	0.045		0.158	
After ground ULF	0.351	0.258		0.906
After GOES ULF			0.150	
After B_z	−0.166	−0.149	−0.230	
After V_x	0.181	0.208	0.385	
After $\sigma V/V$	0.134	0.121		0.170
After $\sigma N/N$	−0.010			
After VLF	0.076	0.087		
After *AE*	−0.092			
After *Kp*				−0.431

[a]Each prediction model is of the form: Predicted Relativistic Electron Flux = Constant + Parameter $_i$ × Observed Value$_i$. (Standardized coefficients have been used in the figures to compare influence of variables.) Predictors and observed values are converted to rankit normal scores [*Sokal and Rohlf*, 1995] by replacing the rank of each observation by the position, in standard deviation units, of the ranked items in a normally distributed sample of the same *n*.

Using these coefficients, we took the 20% of storms held in reserve, predicted the relativistic electron flux following the storm using the independent variables from these storms, and correlated this prediction with the observed flux for each. The observed versus predicted fluxes for both the full and reduced models using ground ULF (no *Kp*) are plotted in Figure 7. The plotted regression line shows the relationship between observed and predicted points.

Correlations between predicted fluxes and observed fluxes are also given for other models in Table 3. The correlation between observed and predicted in all models using ULF is between 0.738 and 0.795. Thus,

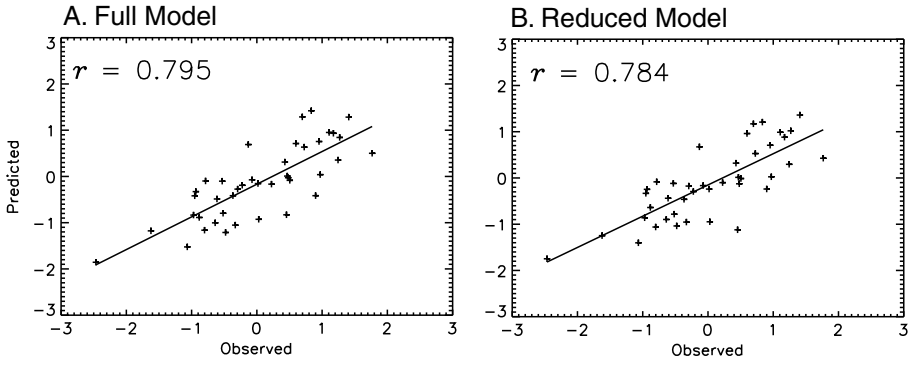

Figure 7. Correlation of flux predicted by ground ULF models (full and reduced) with observed flux in the sample of storms held for validation.

Table 3. Correlations of Predicted Flux With Flux Observed in the Reserved Validation Data Set

Model	Correlation
Ground ULF full Model No *Kp*	0.795
Ground ULF Reduced model No *Kp*	0.784
Ground ULF Reduced model With *Kp*	0.755
GOES ULF Full model No *Kp*	0.785
GOES ULF Reduced model No *Kp*	0.762
GOES ULF Reduced model With *Kp*	0.738
No ULF/with *Kp*[a]	0.729

[a]Although *Kp* was given as a choice, the backward elimination procedure did not retain it. This model's main contributors are seed electrons, after-storm V_x, and after-storm B_z. These parameters, highly correlated with ULF, are explaining part of the variability associated with ULF when ULF is not in the model.

they are all good predictors with little difference in predictive ability. For ground ULF, the best model is the full model without *Kp* (correlation of 0.795), but the reduced model without *Kp* is not far behind (correlation of 0.784). For GOES ULF, the model that correlates best with the observations is the full model (correlation of 0.785).

The addition of *Kp* as a possible predictor slightly lowers the predictive ability of both the ground ULF and GOES ULF models. The attempted "no-ULF" model, which was supposed to showcase the ability of *Kp* to predict without the ULF, is last in predictive ability. As *Kp* was dropped by the backward elimination process, this model, containing neither ULF nor *Kp*, shows a model that could be produced if the ULF index were not available. After-storm V_x and B_z, which are highly correlated with ULF, can take up a good part of the slack in explaining flux, but the addition of ULF still produces a somewhat better prediction.

However, Figure 7 and Table 3 only represent models produced using a particular 80% of the data. Another subset might produce different results. To test this, we also chose various subsets of four fifths of the data, holding one fifth in reserve, and calculated a reduced model for each (using ground ULF). The relative influence of the predictors on flux for each of these data subsets is similar (Figure 8; compare to original data subset in Figure 5a). The percent of variation explained was similar for all reduced models (53%–61%; roughly corresponding to correlations of 0.73–0.78). Main phase seed electrons and ULF, and after-storm ULF were significant in all five data subsets, while the after-storm variation in *V* was significant in four. After-storm V_x was significant in three of the five models, pre-storm flux, and after-storm B_z in two. We also tested the correlation of predictions and observed values for the reduced models (Table 4). The predicted flux from each 80% subset of the data is correlated with the observed flux from the remaining 20% of the data held in reserve for that particular sampling. Correlations between predicted and observed ranged from 0.645 to 0.784 (mean = 0.720). The best of these subsets (the main data subset) was used as the predictive subset in Figure 7.

3.6. Multiple-Predictor Versus Single-Predictor Models

The value of using multiple regression models can be seen if the prediction ability of single predictors is compared to that of multiple-predictor models. Correlations between flux observations and that predicted by selected single variables (Table 5) are consistently lower than the observation-prediction correlations achieved by the multiple regression models. A selection of single predictors for each of the five data subsets are used to produce prediction models. These correlations are averaged over the five data subsets. The three best average correlations are from predictions based solely on ground ULF (0.651), *AE* (0.559), or V_x (0.556). However, even the best of these single-predictor models gives a lower average correlation than that of the regression model predictions.

4. Discussion

The high correlations between the possible predictors of increased relativistic electron flux make it difficult to determine which of these variables best predict flux increases by simple correlation alone. Simple correlations between each predictor and flux give the impression that many possible factors of the IMF and solar wind may be driving flux increases. However, simple correlation analyses cannot tell us whether each parameter is independently correlated with increases in electrons or is only highly correlated with other parameters that are more directly related to electron enhancements. To determine this, more sophisticated methods must be used.

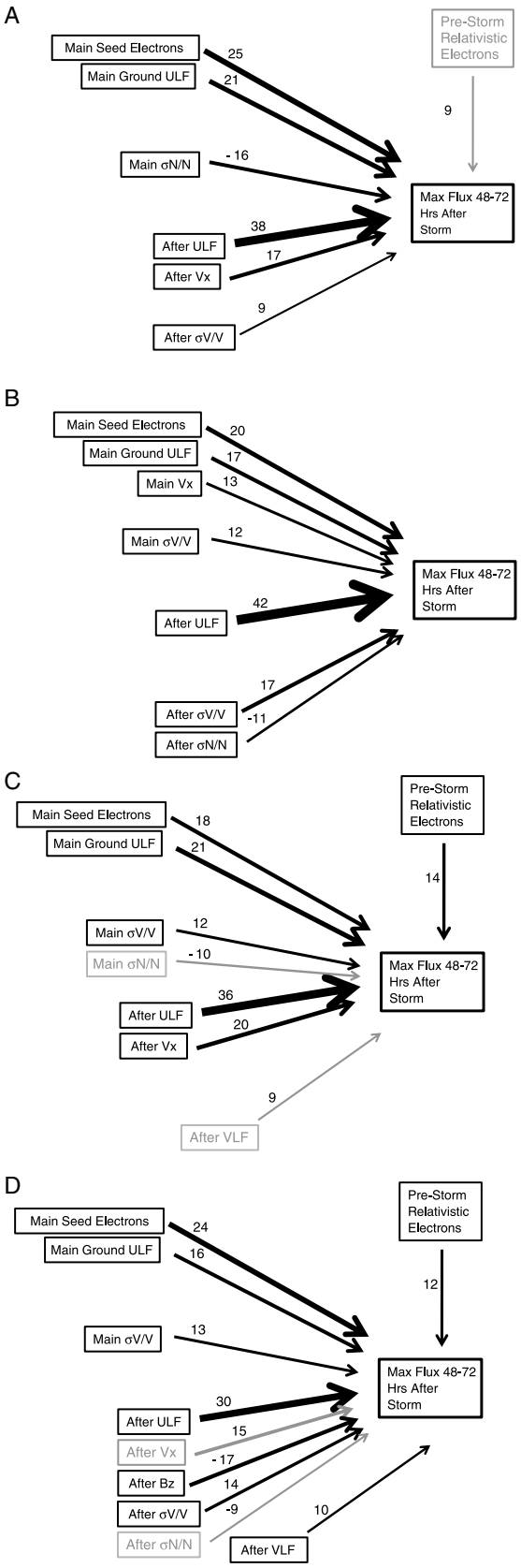

Partial correlations are one method of determining if a variable adds additional influence beyond what other predictors impart, and we have found, in this study, that each predictor loses influence when all other predictors are held constant. However, a more nuanced approach would provide us with information on the relative influence of each parameter and allow the determination of a model that included only those variables that show an effect when others are accounted for. To do this, we have used the method of multiple regression.

4.1. Regression Analyses

The rise in relativistic electron flux following storms is best modeled by a set of variables rather than by one or two factors. The percents of variation explained by the three best single factors individually (after-storm ground ULF, *AE*, and V_x) are 42%, 31%, and 29% (the squared correlation coefficients of 0.65, 0.56, and 0.54, respectively), while a full model explains 59% (roughly, a correlation of 0.77). While ground ULF after the storm may provide a fairly predictive model on its own, predictions could be improved by adding other variables. In addition, studying other variables besides the single highest correlate provides information about the processes at work.

4.2. Full Versus Reduced Models: Determination of a Parsimonious Model

The full model using ground ULF describes 59% of the variation (correlation of 0.77). This is somewhat higher than that described by the reduced models. For this reason, it might appear to be the preferred model for predictive purposes. However, the reduced model might be preferred for several reasons. First, if used for prediction purposes, the full model would

Figure 8. Relative influence of predictors in multiple regression models for four additional subsets of the data. Models use ground ULF and are reduced by backward elimination. Original data subset model is in Figure 6a. All five models are similar in the relative correlation of predictors with flux. Percent variation explained are as follows: (a) 53% ("r" = 0.73), (b) 56% ("r" = 0.75), (c) 59% ("r" = 0.77), and (d) 61% ("r" = 0.78). Sample sizes for the four analyses are as follows: 171, 179, 175, and 174. Factors were removed from the model if the p value was greater than 0.10. Significant predictors ($p < 0.05$) are in black; nonsignificant predictors ($p < 0.10$) are in gray.

Table 4. Correlation of Flux Observations Versus That Predicted From the Reduced Models Derived From Different 80% Subsets of the Data[a]

Data Subset	
A	0.765
B	0.756
C	0.645
D	0.649
Main data set (model in Figure 5)	0.784
Average	0.720

[a]See Figure 8 for models.

necessitate collecting a large amount of mostly irrelevant data. The reduced model would require much less data as input. Second, if used to determine which parameters are most physically meaningful, the reduced model has the advantage. It reduces the explanatory set down to those parameters that can be statistically associated with flux when other parameters are present.

Third, the use of every possible variable increases the risk of problems associated with multicollinearity [*Farrar and Glauber*, 1967]. Very highly correlated predictor variables in a regression model can make calculations of the parameters impossible as the necessary matrix inversions cannot be performed, but even smaller degrees of multicollinearity can make the mathematical results suspect. High correlations between independent variables can make the estimation of their parameters erratic from sample to sample [*Neter et al*., 1985]. The estimates of the coefficients in the model may be unduly influenced by small differences, making the model less robust in its predictions of novel observations. This may not be a problem in using the model for prediction, if the predictions are being made using samples with the same general relationships between the independent variables, but this may not always be the case.

Even if a model with highly correlated predictor variables forecasts future observations well, the estimates of each parameter's influence may be wildly off. If the purpose of a model is only prediction, this may not be of much consequence, but if the model is also being used to test hypotheses about the mechanics of the processes this would invalidate any conclusions drawn. Substantial changes in parameter estimates when variables are highly correlated are certainly seen in our data set. While ULF and the *Kp* index individually show strong positive associations with relativistic electron flux in the simple correlations, the regression models show *Kp* as having a strong negative influence, countered by an even stronger positive effect of ground ULF. This counterintuitive result suggests that ULF and *Kp* are deriving their influence from the same phenomenon and that including both in a model is at best counterproductive. As well, *Kp*, while highly correlated with flux, does not represent a physical quantity. On its own, it may be somewhat useful in predicting flux, but its correlation does not tell us anything about possible mechanisms.

To validate our models, we produced predictions using data from the 20% of storms held in reserve. Predictions of after-storm flux were then correlated with the observed flux for each storm from the reserved data set. All models produced reasonably good predictions, with correlations between predictions and observations ranging from 0.647 to 0.793 (mean correlation of 0.725). Ground ULF and reduced GOES ULF models with *Kp* added were slightly lower in their predictive ability than those without the addition of this index.

Table 5. Correlations of Observed Flux With Flux Predicted From Selected Single Variable Models[a]

Single Predictor	Main Data Subset Validation Set $N = 43$	A $N = 48$	B $N = 40$	C $N = 44$	D $N = 45$	Average Correlation
Onset flux	0.226	0.407	0.388	0.062	0.187	0.254
Seed electron flux	0.247	0.374	0.394	0.383	0.401	0.360
Ground ULF	0.697	0.694	0.726	0.553	0.583	0.651
V_x	0.719	0.647	0.538	0.335	0.546	0.556
B_z	0.371	0.305	0.518	0.459	0.268	0.384
$\sigma N/N$	0.190	0.179	−0.036	0.278	0.006	0.123
$\sigma V/V$	0.181	0.389	0.184	0.195	0.278	0.245
AE	0.530	0.680	0.631	0.468	0.485	0.559
Kp	0.578	0.628	0.644	0.398	0.490	0.548

[a]All variables averaged over the first 48 h following minimum *Dst* except seed electron flux which is measured in the main phase of the storm and onset relativistic electron flux. A different fifth of the data set is held in reserve for each column. A refers to data set used to produce Figure 8a, etc.

Could *Kp* be used without ULF in a predictive model? As it is a more readily available number than the ULF index, a model using *Kp* might be an acceptable substitute. However, a backward elimination model with *Kp* to choose instead of ULF drops the *Kp*, leaving a model where after-storm V_x and B_z, and main phase seed electrons explain most of the variability in flux. The predictive ability of this model is less than that of the model with ULF but might be useful if the ULF index were not available. However, *Kp* is not a useful predictor to add to these models. As a predictor on its own in a single-variable model (Table 5), ULF, V_x, and *AE* all outperform *Kp* in ability to predict flux.

4.3. ULF Effect: Ground Versus Satellite and Narrowband Versus Broadband

Both ground and GOES ULF are correlated with flux increases after storms, but they are also highly correlated with each other—as high as $r = 0.85$ after minimum storm *Dst* (Figure 2). Putting both into a regression model would obscure the overall effect of ULF, so we ran parallel models for each. Their high correlation with each other may tempt us to assume that they are interchangeable, but models run with each are not identical. Ground ULF shows a much stronger association with flux when other variables are added to the model, but the reduced model with GOES ULF shows a stronger effect of B_z after minimum *Dst*. The higher correlation between the ground ULF index and B_z after the storm is responsible for this lowered effect of B_z in the multiple regression.

There are several differences between ground and GOES ULF. The ground ULF index spans only the local daylight hours (local time 0500–1500), while the GOES ULF data cover the full 24 h period. Thus, the ground ULF contains a higher proportion of narrowband ULF, which may be more related to electron acceleration. GOES ULF spans all hours and may therefore be influenced by nighttime substorm activity. However, perhaps the most significant difference between ground and GOES data is that the ground magnetometers, being spread over a wide area at 60° latitude, are better positioned to catch ULF activity. If this activity is confined to a small area, the satellite may simply not be in the right place to see it.

But the percent of variation explained by the models using the ground ULF index is only marginally higher than that using the GOES ULF. Other variables "fill in" when the satellite ULF is not as correlated with the flux increases. For prediction purposes, there may be little reason to favor one over the other. Thus, if only satellite ULF data are available, it would provide an acceptable measure to use in such a model.

ULF activity in the main phase of storms is generally broadband. During recovery (after minimum *Dst*), narrowband waves dominate only in the dawn-noon period [*Posch et al*., 2003]. Therefore, the strong association of relativistic electron flux we see with main phase ULF supports the conclusion that broadband ULF may drive electron acceleration. However, during recovery, the wide longitudinal spread used by the ULF index means both narrowband and broadband ULF will be included. Without more precisely located ULF measurements, it is impossible to determine the association of narrowband activity with flux.

4.4. Initial Conditions and Storm Strength

Neither *AE* nor *Kp* during the pre-storm period shows much correlation with flux in the simple correlations and even less in the full model multiple regressions. The initial conditions, at least as measured by these two indices, do not contribute much to the response of electron flux following the storm. The strength of a storm as measured by the minimum *Dst* and B_z is also of little consequence. Neither of these variables shows much influence in simple correlation. Storm minimum B_z drops out of the reduced models. Only minimum *Dst* remains in the GOES ULF reduced model, where it is one of the less influential variables. Other factors than initial conditions and storm strength are more important in determining flux.

Higher pre-storm relativistic flux shows slightly higher influence in simple correlation, but its effect becomes more pronounced in the multiple regression models, being one of the parameters retained in the reduced models. The population of seed electrons, though, shows an even greater increase in influence when other variables are added. The simple correlation of seed electron flux with accelerated electron flux is not as high as some others (only 0.36), but it is one of the few variables to be included in every reduced model with a fairly high standardized regression coefficient. Whether a storm produces a large flux of relativistic electrons is highly dependent on the seed electron population.

4.5. Comparison to Other Studies

As has been found in other studies, there is little correlation between the strength of a storm and its ability to produce high relativistic electron fluxes [*Reeves et al*., 2003; *Reeves*, 1998]. As the flux following some storms never climbs as high as pre-storm levels [*Onsager et al*., 2002; *O'Brien et al*., 2001], we used pre-storm flux as a predictor of after-storm flux, to be sure that the higher levels after each storm were the result of new generation rather than just the population of electrons that were there to begin with. We discovered that the pre-storm levels were often somewhat predictive of poststorm flux.

We found that the level of seed electrons is a good predictor of relativistic flux following storms, as has previously been mentioned in other studies [*Meredith et al*., 2003; *Hwang et al*., 2004]. Seed electron effect is independent of other processes, as it maintained its influence no matter what other variables were included in the model. *O'Brien and McPherron* [2003] suggested that enhancement of the seed electron population associated with magnetic storms was responsible for the increase in ULF waves which then resulted in acceleration of relativistic electrons.

The average IMF B_z after the storm is commonly found to be an important correlate with flux [*Blake et al*., 1997; *Iles et al*., 2002; *Miyoshi and Kataoka*, 2008; *Miyoshi et al*., 2013]. We found a moderate simple correlation of this variable with flux, but its effect was reduced by the introduction of other variables in the overall analyses.

Although previous studies have shown a negative correlation with number density, our variable N Shock (the maximum N seen during pre-storm or main phase) showed no correlation at all with flux. Main phase $\sigma N/N$, although retained in the reduced model, generally had only a modest, nonsignificant correlation with flux after storms.

Electric field and pressure have been found to be important [*Tan et al*., 2011]. In our study, the simple correlation of flux with pressure, while significant, is not as high as that of other variables, and in the partial correlations, its effect drops nearly to zero. Given this, and as it is highly correlated with several other variables, we do not test it in the multiple regression models. We do find a strong simple correlation of flux with E_y which is still high even in the partial correlations (simple correlation = 0.420, partial correlation = 0.263). We might have retained E_y in the regression models except for the fact that it is highly correlated with the parameter from which it is derived: IMF B_z. Only one of E_y or IMF B_z could be retained in the model.

Several studies have found that the *AE* index, a measure of substorm activity, is related to increased flux following storms. In our study, the *AE* following the storm was a significant factor if GOES ULF was used. When ground ULF was used, the *AE* influence was less pronounced. There is a high correlation between *AE* and ULF. This may be an indication that substorm activity is a strong driver of ULF activity or only that the two indices are a reflection of a generalized ground magnetometer activity.

VLF and ULF waves are thought to be the primary sources of energy for either accelerating electrons or transporting high-energy electrons. Our study confirms the possible role of ULF waves. Further, we show that ULF waves have a strong effect independent of other parameters with which they are strongly correlated. Whether the ULF activity was measured on the ground or by satellite, it consistently remained one of the major correlates of flux. Based on a model, *O'Brien and McPherron* [2003] proposed that the effect of ULF wave power would be enhanced by the stronger *Dst* associated with storms. Our empirical study only supports this idea for satellite ULF, where the minimum storm *Dst* remains in the reduced model as a weaker predictor. Our reduced model using the ground ULF index showed no influence of the *Dst* level on electron enhancements.

Ground-based VLF activity, however, showed little ability to predict future flux in our models, even in the simple correlations, although a previous statistical study reported an association of flux with ground-observed VLF waves [*Smith et al*., 2004]. As well, satellite observations show this association in both statistical studies [*Meredith et al*., 2003; *O'Brien et al*., 2003; *Horne et al*., 2005; *Miyoshi et al*., 2013] and in recent observations of the concomitant time evolution of VLF waves and flux enhancements during storms [*Horne et al*., 2005; *Thorne et al*., 2013; *Li et al*., 2014; *Su et al*., 2014; *Turner et al*., 2014; *Xiao et al*., 2014].

The difficulty we have found in predicting flux enhancements using VLF waves may be due to several issues. First, in previous studies, we note that VLF wave power rises nearly simultaneously with relativistic electron flux. Our approach of predicting flux with VLF waves measured a day or more before the flux rise

AGU Journal of Geophysical Research: Space Physics 10.1002/2014JA019955

Table 6. Predictors Found to Be Correlated With Flux in Previous Studies and in the Multiple Regressions of the Present Study[a]

	Previous Studies		Current Study (Storms Only)	
	Yearlong	Storms Only	Ground ULF	GOES ULF
Storm minimum *Dst*		(No effect [*Reeves et al.*, 2003; *Reeves*, 1998])	*N*	*N*
Storm minimum B_z			*N*	*N*
AE		*Baker et al.* [1990], *Meredith et al.* [2003], and *Li et al.* [2009]	*N*	*Y*
Kp			*Y*[b]	*Y*[b]
V_x (Solar wind velocity)	*Paulikas and Blake* [1979], *Blake et al.* [1997], *Baker et al.* [1998b], *Ukhorskiy et al.* [2004], *Lyatsky and Khazanov* [2008a, 2008b], *Reeves et al.* [2011], *Kellerman and Shprits* [2012], *Potapov et al.* [2012], and *Potapov et al.* [2014]	*O'Brien et al.* [2001], *Reeves et al.* [2003], and *Lyons et al.* [2005]	*Y*	*Y*
$\sigma V/V$ (variation in *V*/magnitude of *V*)	*Potapov et al.* [2012]		*Y*	*N*
N	Negative correlation: *Lyatsky and Khazanov* [2008b], *Balikhin et al.* [2011], *Kellerman and Shprits* [2012], and *Potapov et al.* [2012]		*N*	*N*
$\sigma N/N$ (variation in *N*/magnitude of *N*)			*S*	*S*
ULF	*Potapov et al.* [2014]	*Rostoker et al.* [1998], *Mathie and Mann* [2000], *O'Brien et al.* [2003], *Kozyreva et al.* [2007], *Tan et al.* [2004], *Tan et al.* [2011], and *Clausen et al.* [2011]	*Y*	*Y*
VLF		Satellite: *Meredith et al.* [2003], *O'Brien et al.* [2003], and *Miyoshi et al.* [2013]; Ground: *Lyons et al.* [2005] and *Smith et al.* [2004]	*S*	*N*
After-storm B_z		*Blake et al.* [1997], *Iles et al.* [2002], *Miyoshi and Kataoka* [2008], and *Miyoshi et al.* [2013]	*Y*	*Y*
Pre-storm relativistic flux		*Reeves et al.* [2003]	*S*	*S*
Seed electron flux		*Hwang et al.* [2004]	*Y*	*Y*

[a] *Y* = correlated with flux. *N* = not correlated with flux. *S* = minor correlation with flux ($0.05 < P < .10$).
[b] *Kp* was not tested in all models.

would miss this correlation. Second, the Halley 1.0 kHz VELOX channel, corresponding to an L_{max} of 7.52 (including all $L < 7.52$) [*Smith*, 1995; *Smith et al*., 2004], includes the frequency of the expected peak of lower band chorus power near geostationary orbit (~0.3 Ω_e). Indeed, *Smith et al*. [2004] found that events with high relativistic electron flux at geostationary orbit were associated with higher after-storm ground VLF power in the 0.5 kHz and 1.0 kHz channels ($L < 9.47$ and $L < 7.52$, respectively) but found an anticorrelation with higher after-storm power in 4.25 kHz channel ($L < 4.64$). The positive association found by *Smith et al*. [2004] for the 0.5 and 1.0 kHz channels is consistent with the low, but not zero, correlation we have found between VLF power in the 1.0 kHz channel and geostationary relativistic electron flux. We did not have access to long-term satellite VLF data from geostationary orbit, but we were hopeful that ground VLF would correlate well enough with satellite VLF observations to provide decent predictive capability. This does not appear to be the case. The recent observations from the Van Allen Probes of strong correlations between VLF chorus and relativistic electron fluxes at L shells lower than those of geostationary orbit [*Thorne et al*., 2013] suggest that the influence of VLF chorus is strongly L dependent, with electron acceleration due to VLF waves occurring at L shells inside of geostationary orbit. (ULF wave power, on the other hand, may still show a strong association because the role of ULF waves is to transport the resultant relativistic fluxes out toward the geostationary satellite instrumentation.) The location of Halley at $L \sim 4.5$ means that the VLF waves observed by VELOX are dominated by those originating from closer to the receiver than the L shell of geostationary satellites. Third, the penetration of VLF waves to the ground is influenced by the state of the ionosphere and the levels of solar illumination. In the summer months, VLF amplitude in the 1–3 kHz range is reduced due to this attenuation effect [*Smith*, 2010]. Thus, the predictive ability of VLF waves may be significantly lowered during these time periods when the measured amplitude is reduced, and ground VLF would not necessarily be well coupled with satellite VLF from the same L shell. These questions are explored further in a separate paper (L. E. Simms et al., Prediction of relativistic electron flux at geostationary orbit using VLF waves, submitted to *Journal of Geophysical Research*, 2014).

Smith et al. [2004] also found an association between pre-storm ground-based VLF and flux. Our initial correlation analysis found a small correlation between pre-storm VLF and after-storm flux, as well as between pre-storm ULF and after-storm flux. However, neither VLF nor ULF in the pre-storm period was significant in predicting after-storm flux in the regression models.

Previous studies have tended to find more significant correlates than our present study (Table 6). This is likely due to the use of simple correlation analysis in many studies. Some predictors are less influential when whole years are considered. As will be shown in a future paper, the influence of ULF drops markedly in a full year analysis, while $\sigma N/N$ shows a strong negative correlation (L. E. Simms et al., Day to day predictive models of relativistic electron flux at geostationary orbit: Multiple regression analysis, submitted to *Journal of Geophysical Research*, 2014). Previous studies that found a correlation of ULF with flux were also done only in disturbed times (Table 6).

These correlation studies, while they do not prove a cause-effect relationship between a predictor and flux, do allow us to develop and possibly disprove hypotheses about which variables may be important drivers. Simple correlations between predictors and flux, however, are of less value in disproving hypotheses than multiple regression analyses, due to the intercorrelation of predictor variables. A variable that shows no correlation to flux is less likely to be a physical process that drives the flux increases. However, a lack of correlation may be due to measurement choices, as evidenced by the difficulty we experienced in finding a predictive relationship between VLF waves and relativistic electron flux.

5. Summary

The prediction of relativistic electron flux is accomplished in our study by determining the parameters of a multiple regression model. We produce several such models: full models using all variables we have access to, as well as parsimonious models with only those parameters necessary to explain the observed variance in the independent variable. We produced models both with and without the *Kp* index to see if its effect only duplicated that of the physical variables of the solar wind and IMF. The predictions from all of these various models were well correlated with observations from data we held in reserve for validation purposes.

The predictive power of each variable may depend on how it is measured (e.g., ground versus space for ULF), what other variables are included or excluded from the model, and the training period for the analysis. As a

consequence, the best predictor is not necessarily the major driver of radiation belt dynamics. However, it is likely that tested predictors which consistently fail to show an effect are not significant drivers of flux increases. We recommend that these techniques be employed in future statistical studies using relativistic electron flux data obtained at lower L shells, such as that currently being obtained by the Van Allen Probes.

Acknowledgments

Relativistic electron and seed electron flux data were obtained from Los Alamos National Laboratory (LANL) geosynchronous energetic particle instruments (contact G.D. Reeves). Satellite and ground-based ULF indices are available at http://virbo.org/Augsburg/ULF and Halley VLF VELOX data at http://bsauasc.nerc-bas.ac.uk:8080/~pdata/velox_summary/. B_z, V, N, P, σV, σN, and Kp, Dst, and AE indices are available from Goddard Space Flight Center Space Physics Data Facility at the OMNIWeb data website (http://omniweb.gsfc.nasa.gov/html/ow_data.html). We thank the referees for their helpful comments. This work was supported by National Science Foundation grant ATM-0827903 to Augsburg College.

Michael Balikhin thanks the reviewers for their assistance in evaluating this paper.

References

Albert, J. M., N. P. Meredith, and R. B. Horne (2009), Three-dimensional diffusion simulation of outer radiation belt electrons during the 9 October 1990 magnetic storm, *J. Geophys. Res.*, *114*, A09214, doi:10.1029/2009JA014336.

Baker, D. N., R. D. Belian, P. R. Higbie, R. W. Kebesadel, and J. B. Blake (1987), Deep dielectric charging effects due to high energy electrons in the Earth's outer magnetosphere, *J. Electrost.*, *20*, 3–19.

Baker, D. N., R. L. McPherron, T. E. Cayton, and R. W. Klebesadel (1990), Linear prediction filter analysis of relativistic electron properties at 6.6 RE, *J. Geophys. Res.*, *95*(A9), 15,133–15,140, doi:10.1029/JA095iA09p15133.

Baker, D. N., J. H. Allen, S. G. Kanekal, and G. D. Reeves (1998a), Disturbed space environment may have been related to pager satellite failure, *Eos Trans. AGU*, *79*, 477–492, doi:10.1029/98EO00359.

Baker, D. N., X. Li, J. B. Blake, and S. Kanekal (1998b), Strong electron acceleration in the Earth's magnetosphere, *Adv. Space Res.*, *21*(4), 609–613.

Balikhin, M. A., R. J. Boynton, S. N. Walker, J. E. Borovsky, S. A. Billings, and H. L. Wei (2011), Using the NARMAX approach to model the evolution of energetic electrons fluxes at geostationary orbit, *Geophys. Res. Lett.*, *38*, L18105, doi:10.1029/2011GL048980.

Blake, J. B., D. N. Baker, N. Turner, K. W. Ogilvie, and R. P. Lepping (1997), Correlation of changes in the outer-zone relativistic-electron population with upstream solar wind and magnetic field measurements, *Geophys. Res. Lett.*, *24*(8), 927–929, doi:10.1029/97GL00859.

Chatterjee, S., A. S. Hadi, and B. Price (2000), *Regression by Example*, 3rd ed., Wiley-Interscience, New York.

Clausen, L. B. N., J. B. H. Baker, J. M. Ruohoniemi, and H. J. Singer (2011), ULF wave characteristics at geosynchronous orbit during the recovery phase of geomagnetic storms associated with strong electron acceleration, *J. Geophys. Res.*, *116*, A09203, doi:10.1029/2011JA016666.

Dmitriev, A. V., and J. K. Chao (2003), Dependence of geosynchronous relativistic electron enhancements on geomagnetic parameters, *J. Geophys. Res.*, *108*(A11), 1388, doi:10.1029/2002JA009664.

Elkington, S. R. (2006), A review of ULF interactions with radiation belt electrons, in *Solar Eruptions and Energetic Particles*, *Geophys. Monogr. Ser.*, vol. 165, AGU, Washington, D. C., doi:10.1029/165GM12.

Farrar, D. E., and R. R. Glauber (1967), "Multicollinearity in regression analysis: The problem revisited," *Rev. Econ. Stat. 49*(1), 92–107.

Golden, D. I., M. Spasojevic, W. Li, and Y. Nishimura (2012), Statistical modeling of plasmaspheric hiss amplitude using solar wind measurements and geomagnetic indices, *Geophys. Res. Lett.*, *39*, L06103, doi:10.1029/2012GL051185.

Green, J. C., and M. G. Kivelson (2001), A tale of two theories: How the adiabatic response and ULF waves affect relativistic electrons, *J. Geophys. Res.*, *106*(A11), 25,777–25,791, doi:10.1029/2001JA000054.

Hocking, R. R. (1976), The analysis and selection of variables in linear regression, *Biometrics*, *32*, 1–49.

Horne, R. B., R. M. Thorne, S. A. Glauert, J. M. Albert, N. P. Meredith, and R. R. Anderson (2005), Timescale for radiation belt electron acceleration by whistler mode chorus waves, *J. Geophys. Res.*, *110*, A03225, doi:10.1029/2004JA010811.

Hwang, J., K. W. Min, E. Lee, C. Lee, and D. Y. Lee (2004), A case study to determine the relationship of relativistic electron events to substorm injections and ULF power, *Geophys. Res. Lett.*, *31*, L23801, doi:10.1029/2004GL021544.

Iles, R. H. A., A. N. Fazakerley, A. D. Johnstone, N. P. Meredith, and P. Buhler (2002), The relativistic electron response in the outer radiation belt during magnetic storms, *Ann. Geophys.*, *20*, 957.

Kellerman, A. C., and Y. Y. Shprits (2012), On the influence of solar wind conditions on the outer-electron radiation belt, *J. Geophys. Res.*, *117*, A05217, doi:10.1029/2011JA017253.

Kim, H.-J., and A. A. Chan (1997), Fully adiabatic changes in storm time relativistic electron fluxes, *J. Geophys. Res.*, *102*(A10), 22,107–22,116, doi:10.1029/97JA01814.

Kozyreva, O. V., V. A. Pilipenko, M. J. Engebretson, and K. Yumoto (2007), A new ULF wave index and its comparison with dynamics of geostationary relativistic electrons, *Planet. Space Sci.*, *55*, 755–769.

Lanzerotti, L. J. (2001), Space weather effects on communications, in *Space Storms and Space Weather Hazards*, NATO Sci. Ser. II: Mathematics, Physics and Chemistry, vol. 38, edited by I. Daglis, pp. 313, Kluwer Acad., Norwell, Mass.

Li, L. Y., J. B. Cao, G. C. Zhou, and X. Li (2009), Statistical roles of storms and substorms in changing the entire outer zone relativistic electron population, *J. Geophys. Res.*, *114*, A12214, doi:10.1029/2009JA014333.

Li, W., et al. (2014), Radiation belt electron acceleration by chorus waves during the 17 March 2013 storm, *J. Geophys. Res. Space Physics*, *119*, doi:10.1002/2014JA019945.

Li, X., M. Temerin, D. N. Baker, G. D. Reeves, and D. Larson (2001), Quantitative prediction of radiation belt electrons at geostationary orbit based on solar wind measurements, *Geophys. Res. Lett.*, *28*, 1887–1890, doi:10.1029/2000GL012681.

Li, X., M. Temerin, D. N. Baker, and G. D. Reeves (2011), Behavior of MeV electrons at geosynchronous orbit during last two solar cycles, *J. Geophys. Res.*, *116*, A11207, doi:10.1029/2011JA016934.

Lyatsky, W., and G. V. Khazanov (2008a), Effect of solar wind density on relativistic electrons at geosynchronous orbit, *Geophys. Res. Lett.*, *35*, L03109, doi:10.1029/2007GL032524.

Lyatsky, W., and G. V. Khazanov (2008b), Effect of geomagnetic disturbances and solar wind density on relativistic electrons at geostationary orbit, *J. Geophys. Res.*, *113*, A08224, doi:10.1029/2008JA013048.

Lyons, L. R., D.-Y. Lee, R. M. Thorne, R. B. Horne, and A. J. Smith (2005), Solar wind-magnetosphere coupling leading to relativistic electron energization during high-speed streams, *J. Geophys. Res.*, *110*, A11202, doi:10.1029/2005JA011254.

Mathie, R. A., and I. R. Mann (2000), A correlation between extended intervals of ULF wave power and storm-time geosynchronous relativistic electron flux enhancements, *Geophys. Res. Lett.*, *27*(20), 3261–3264, doi:10.1029/2000GL003822.

Meredith, N. P., M. Cain, R. B. Horne, R. M. Thorne, D. Summers, and R. R. Anderson (2003), Evidence for chorus-driven electron acceleration to relativistic energies from a survey of geomagnetically disturbed periods, *J. Geophys. Res.*, *108*(A6), 1248, doi:10.1029/2002JA009764.

Miyoshi, Y., and R. Kataoka (2008), Flux enhancement of the outer radiation belt electrons after the arrival of stream interaction regions, *J. Geophys. Res.*, *113*, A03S09, doi:10.1029/2007JA012506.

Miyoshi, Y., R. Kataoka, Y. Kasahara, A. Kumamoto, T. Nagai, and M. F. Thomsen (2013), High-speed solar wind with southward interplanetary magnetic field causes relativistic electron flux enhancement of the outer radiation belt via enhanced condition of whistler waves, *Geophys. Res. Lett.*, *40*, 4520–4525, doi:10.1002/grl.50916.

Neter, J., W. Wasserman, and M. H. Kutner (1985), *Applied Linear Statistical Models*, pp. 1127, Richard D. Irwin, Inc, Homewood, Ill.
O'Brien, T. P., and R. L. McPherron (2003), An empirical dynamic equation for energetic electrons at geosynchronous orbit, *J. Geophys. Res.*, *108*(A3), 1137, doi:10.1029/2002JA009324.
O'Brien, T. P., R. L. McPherron, D. Sornette, G. D. Reeves, R. Friedel, and H. J. Singer (2001), Which magnetic storms produce relativistic electrons at geosynchronous orbit?, *J. Geophys. Res.*, *106*(A8), 15,533–15,54A4, doi:10.1029/2001JA000052.
O'Brien, T. P., K. R. Lorentzen, I. R. Mann, N. P. Meredith, J. B. Blake, J. F. Fennell, M. D. Looper, D. K. Milling, and R. R. Anderson (2003), Energization of relativistic electrons in the presence of ULF power and MeV microbursts: Evidence for dual ULF and VLF acceleration, *J. Geophys. Res.*, *108*(A8), 1329, doi:10.1029/2002JA009784.
Onsager, T. G., G. Rostoker, H.-J. Kim, G. D. Reeves, T. Obara, H. J. Singer, and C. Smithtro (2002), Radiation belt electron flux dropouts: Local time, radial, and particle-energy dependence, *J. Geophys. Res.*, *107*(A11), 1382, doi:10.1029/2001JA000187.
Paulikas, G. A., and J. B. Blake (1979), Effects of the solar wind on magnetospheric dynamics: Energetic electrons at the synchronous orbit, in *Quantitative Modeling of Magnetospheric Processes*, *Geophys. Monogr. Ser.*, vol. 21, pp. 180–202, AGU, Washington, D. C.
Pilipenko, V., N. Yagova, N. Romanova, and J. Allen (2006), Statistical relationships between satellite anomalies at geostationary orbit and high-energy particles, *Adv. Space Res.*, *37*, 1192–1205.
Posch, J. L., M. J. Engebretson, V. A. Pilipenko, W. J. Hughes, C. T. Russell, and L. J. Lanzerotti (2003), Characterizing the long-period ULF response to magnetic storms, *J. Geophys. Res.*, *108*(A1), 1029, doi:10.1029/2002JA009386.
Potapov, A. S., B. Tsegmed, and L. V. Ryzhakova (2012), Relationship between the fluxes of relativistic electrons at geosynchronous orbit and the level of ULF activity on the Earth's surface and in the solar wind during the 23rd solar activity cycle, *Cosmic Research*, *50*(2), 124–140.
Potapov, A. S., B. Tsegmed, and L. V. Ryzhakova (2014), Solar cycle variation of "killer" electrons at geosynchronous orbit and electron flux correlation with the solar wind parameters and ULF waves intensity, *Acta Astronaut.*, *93*, 55–63.
Reeves, G. D. (1998), Relativistic electrons and magnetic storms: 1992–1995, *Geophys. Res. Lett.*, *25*(11), 1817–1820, doi:10.1029/98GL01398.
Reeves, G. D., R. H. W. Friedel, R. D. Belian, M. M. Meier, M. G. Henderson, T. Onsager, H. J. Singer, D. N. Baker, X. Li, and J. B. Blake (1998), The relativistic electron response at geosynchronous orbit during the January 1997 magnetic storm, *J. Geophys. Res.*, *103*(A8), 17,559–17,570, doi:10.1029/97JA03236.
Reeves, G. D., K. L. McAdams, and R. H. W. Friedel (2003), Acceleration and loss of relativistic electrons during geomagnetic storms, *Geophys. Res. Lett.*, *30*(10), 1529, doi:10.1029/2002GL016513.
Reeves, G. D., S. K. Morley, R. H. W. Friedel, M. G. Henderson, T. E. Cayton, G. Cunningham, J. B. Blake, R. A. Christensen, and D. Thomsen (2011), On the relationship between relativistic electron flux and solar wind velocity: Paulikas and Blake revisited, *J. Geophys. Res.*, *116*, A02213, doi:10.1029/2010JA015735.
Rostoker, G., S. Skone, and D. N. Baker (1998), On the origin of relativistic electrons in the magnetosphere associated with some geomagnetic storms, *Geophys. Res. Lett.*, *25*(19), 3701–3704, doi:10.1029/98GL02801.
Simms, L. E., V. A. Pilipenko, and M. J. Engebretson (2010), Determining the key drivers of magnetospheric Pc5 wave power, *J. Geophys. Res.*, *115*, A10241, doi:10.1029/2009JA015025.
Smith, A. J. (1995), VELOX: A new VLF/ELF receiver in Antarctica for the Global Geospace Science mission, *J. Atmos. Terr. Phys.*, *57*(5), 507–524.
Smith, A. J. (2010), The statistics of natural ELF/VLF waves derived from a long continuous set of ground-based observations at high latitude, *J. Atmos. Terr. Phys.*, *72*, 463–475.
Smith, A. J., N. P. Meredith, and T. P. O'Brien (2004), Differences in ground-observed chorus in geomagnetic storms with and without enhanced relativistic electron fluxes, *J. Geophys. Res.*, *109*, A11204, doi:10.1029/2004JA010491.
Sokal, R. R., and F. J. Rohlf (1995), *Biometry: The Principles and Practice of Statistics in Biological Research*, 3rd ed., pp. 859, W.H. Freeman, New York.
Su, Z., et al. (2014), Intense duskside lower band chorus waves observed by Van Allen Probes: Generation and potential acceleration effect on radiation belt electrons, *J. Geophys. Res. Space Physics*, *119*, 4266–4273, doi:10.1002/2014JA019919.
Tan, L. C., S. F. Fung, and X. Shao (2004), Observation of magnetospheric relativistic electrons accelerated by Pc-5 ULF waves, *Geophys. Res. Lett.*, *31*, L14802, doi:10.1029/2004GL019459.
Tan, L. C., X. Shao, A. S. Sharma, and S. F. Fung (2011), Relativistic electron acceleration by compressional-mode ULF waves: Evidence from correlated Cluster, Los Alamos National Laboratory spacecraft, and ground-based magnetometer measurements, *J. Geophys. Res.*, *116*, A07226, doi:10.1029/2010JA016226.
Thorne, R. M., et al. (2013), Rapid local acceleration of relativistic radiation-belt electrons by magnetospheric chorus, *Nature*, *504*, 411, doi:10.1038/nature12889.
Tu, W., G. S. Cunningham, Y. Chen, S. K. Morley, G. D. Reeves, J. B. Blake, D. N. Baker, and H. Spence (2014), Event-specific chorus wave and electron seed population models in DREAM3D using the Van Allen Probes, *Geophys. Res. Lett.*, *41*, 1359–1366, doi:10.1002/2013GL058819.
Turner, D. L., et al. (2014), Competing source and loss mechanisms due to wave-particle interactions in Earth's outer radiation belt during the 30 September to 3 October 2012 geomagnetic storm, *J. Geophys. Res. Space Physics*, *119*, 1960–1979, doi:10.1002/2014JA019770.
Ukhorskiy, A. Y., M. I. Sitnov, A. S. Sharma, B. J. Anderson, S. Ohtani, and A. T. Y. Lui (2004), Data-derived forecasting model for relativistic electron intensity at geosynchronous orbit, *Geophys. Res. Lett.*, *31*, L09806, doi:10.1029/2004GL019616.
Vassiliadis, D., A. J. Klimas, S. G. Kanekal, D. N. Baker, and R. S. Weigel (2002), Long-term-average, solar cycle, and seasonal response of magnetospheric energetic electrons to the solar wind speed, *J. Geophys. Res.*, *107*(A11), 1383, doi:10.1029/2001JA000506.
Weigel, R. S., A. J. Klimas, and D. Vassiliadis (2003), Precursor analysis and prediction of large-amplitude relativistic electron fluxes, *Space Weather*, *1*(3), 1014, doi:10.1029/2003SW000023.
Xiao, F., et al. (2014), Chorus acceleration of radiation belt relativistic electrons during March 2013 geomagnetic storm, *J. Geophys. Res. Space Physics*, *119*, 3325–3332, doi:10.1002/2014JA019822.